

## Article

# Study of Mechanical Properties of Saline Soils under Different Stress Paths

Shukai Cheng<sup>1</sup>, Qing Wang<sup>2,\*</sup>, Jiaqi Wang<sup>3</sup> and Yan Han<sup>2</sup>

<sup>1</sup> School of Civil Engineering and Architecture, Henan University of Science and Technology, Luoyang 471000, China

<sup>2</sup> College of Construction Engineering, Jilin University, Changchun 130026, China

<sup>3</sup> School of Civil Engineering, Changchun Institute of Technology, Changchun 130012, China

\* Correspondence: wangqing@jlu.edu.cn

**Abstract:** The stress path is a critical factor affecting the mechanical properties of saline soils. In order to study the mechanical properties of saline soils under different stress paths, in situ saline soils in the Qian'an area of western Jilin province were selected for this study, and triaxial shear tests under six different stress paths were conducted, including the consolidated undrained triaxial test under the conventional stress path under the isobaric consolidation condition; the consolidated drained triaxial test under the conventional, equal  $p$ , reduced  $p$ , and increased  $p$  stress paths under the isobaric consolidation condition; and the consolidated drained triaxial test under the conventional stress path under the  $K_0$  consolidation condition. The effects of the consolidation conditions, drainage conditions, and stress paths on the mechanical properties of in situ saline soils were investigated. The results reveal that the stress–strain relationship curves of soil samples decrease continuously in the order of increased  $p$ , conventional, equal  $p$ , and decreased  $p$ , and they all show the characteristics of strain hardening. The stress path curves have the same slope under the same stress path. For different confining pressures, only the relative positions of the curves are different. Under the conventional stress path, the slope is 1; under the increased  $p$  stress path, the slope is 1/3; under the equal  $p$  stress path, the slope is 3; and under the decreased  $p$  stress path, the slope of the curve is  $-1$ . For the same confining pressure, the magnitude relationships of shear strength under the different stress paths are as follows: increased  $p >$  conventional  $>$  equal  $p >$  decreased  $p$ . For the cohesion  $c$  and internal friction angle  $\varphi$ , the consolidation condition has a greater effect on the cohesion  $c$  and a smaller effect on the internal friction angle  $\varphi$ ; the drainage condition has a smaller effect on the cohesion  $c$  and a larger effect on the internal friction angle  $\varphi$ ; and the stress paths have a greater effect on both cohesion  $c$  and internal friction angle  $\varphi$ .

**Keywords:** stress–strain relationship; shear strength parameters; in situ soil sample; triaxial shear test; mechanical properties



**Citation:** Cheng, S.; Wang, Q.; Wang, J.; Han, Y. Study of Mechanical Properties of Saline Soils under Different Stress Paths. *Buildings* **2023**, *13*, 2347. <https://doi.org/10.3390/buildings13092347>

Academic Editors: Yong Tan, Xudong Zhang, Bingxiang Yuan, Yong Liu and Yonghong Wang

Received: 28 June 2023

Revised: 19 August 2023

Accepted: 13 September 2023

Published: 15 September 2023



**Copyright:** © 2023 by the authors. Licensee MDPI, Basel, Switzerland. This article is an open access article distributed under the terms and conditions of the Creative Commons Attribution (CC BY) license (<https://creativecommons.org/licenses/by/4.0/>).

## 1. Introduction

The mechanical properties of the soil not only depend on the nature of the soil itself but also are affected by the stress state, stress path, and other factors, so the engineering construction project should try to choose the stress path that can truly reflect the soil stress state, loading method, and drainage conditions for the test [1]. With the development of railways, highways, power stations, and diversion irrigation projects, saline soil in cold regions is widely used as the foundation and structure of engineering construction projects [2–6]. Deep research into the effects of stress path on soil deformation and strength characteristics is of great significance to the design and maintenance of these projects [7–12].

In 1967, Lamber [13] defined the concept of stress paths and proposed that the deformation and strength properties of soils under different stress paths could be investigated using the stress path method (SPM). Triaxial tests can be performed for a variety of different

stress paths, usually with increasing, decreasing, or constant confining pressure or mean principal stresses to study the differences in the deformation and strength of various types of soils under different stress paths [14–16]. For different types of soils, many experts and scholars have studied the mechanical properties under different stress paths.

In the initial research phase, the main study referenced was on the mechanical properties of stress paths in cohesionless soils such as sandy soils [17–19]. Breth and Schuster [20] point out that the mechanical properties of the soil are strongly influenced by the stress path. Xu and Wen [21] found that the shear dilatation of sandy soil was greater under compression than under tension, and the shear dilatation decreased under decompression compression, conventional compression, and increased compression, in that order. With the progress of research and the needs of engineering construction, research on stress paths in cohesive soils has received more and more attention, and significant progress has been made in recent years. Silvestri and Diab [22] proposed a new analytical method for the interpretation of pressuremeter tests in clay soils, where the total and effective stress paths followed by deformation in the soil can be represented on a shear stress–normal stress diagram. Chang and Wang [23] studied the mechanical properties of in situ clay under different stress paths and found that the stress–strain relationships of the soils under different stress paths all showed a nonlinear strain-hardening type with similar curve patterns. Liu and Shi [24] and Kong and Zang [25] conducted laboratory tests on in situ and remoulded clays under various stress paths to reveal the mechanical properties of structural in situ soils under different stress paths. Wang and Chen [26] studied the stress–strain characteristics of silty clay under multiple stress paths by examining the stress path characteristics of pit excavation. Huang and Liu [27] conducted an experimental study on the stress paths of saturated soft clay at different temperatures. As a special soil that is widely studied, many scholars have also conducted many studies on the mechanical properties of stress paths in loess. Shi and Liu [28] conducted triaxial tests under equal stress ratio and conventional conditions and analysed the effects of the two stress paths on the mechanical properties of loess. Liang and Xie [29] investigated the effect of stress paths on the consolidated undrained shear strength of Longxi Q3 in situ loess using the total stress method. Jiang and Hu [30] conducted triaxial compression tests on remoulded and in situ loess under an equal  $p$  stress path, conventional stress path, and reduced  $p$  stress path, and the pore distribution inside the soil before and after the test was measured using the mercury intrusion test, and the relationship between the mechanical properties and pores was analysed. Using the mercury intrusion test, Hu and Jiang [31] compared the pore characteristics of the initial specimens of loess and the specimens after experiencing different stress paths and investigated the fractal dimensions of the pores. Hou and Li [32] investigated the damage mechanism of loess slopes using stress path tests. Zhao and Fu [33] explored the mechanical properties of saturated remoulded loess under vertical loading and an equal shear path. Many other experts and scholars have made certain analyses and studies on the mechanical properties and intrinsic relationships of granular soils [34], reinforced soils [35], fly ash [36], rock piles [37], concrete [38], sandstone [39], red clay [16], and calcareous sand [40] under different stress paths.

Saline soil is a regional special soil. For a long time, most studies on the mechanical properties of saline soil have been based on conventional triaxial tests under isotropic isobaric conditions. In fact, the mechanical properties of saline soil are related to the engineering construction working conditions, and the stress–strain relationship varies in different parts of the soil with different stress paths. Therefore, it is important to conduct experimental research based on the stress path experienced by the soil in engineering construction projects to obtain reliable test parameters to ensure the safety of the projects. Carbonated saline soils are widely distributed in western Jilin province, China, and many studies have been carried out on carbonated saline soil. Wang and Kong [41] proposed that the saline soil there is a structural soil. In terms of dispersion, Bao and Wang [42] and Zhang and Wang [43] researched the dispersion properties of the area and considered the saline soil in the area a dispersion saline soil. In terms of mechanical properties, Han and

Wang [44] studied the action of freeze–thaw cycles on the unconsolidated undrained shear strength of saline soil in western Jilin province, China.

In engineering construction projects, the different construction methods and construction properties of the project, etc., all lead to changes in the stress state of the saline soil, which experiences different stress paths in different parts of the soil during the construction process. The study of the mechanical properties of saline soils under different stress paths can provide some reference basis for guiding actual engineering construction, although there are fewer studies on the mechanical properties of carbonate saline soils under different stress path conditions. Therefore, this study takes in situ saline soil in Qian'an (in western Jilin province, China) as its object, and triaxial laboratory tests were conducted on in situ saline soils under different consolidation conditions, different drainage conditions, and different stress path conditions using a GDS unsaturated triaxial apparatus to investigate the effects of different stress paths, drainage conditions, and consolidation states on the mechanical properties of saline soils.

## 2. Materials and Experimental Program

### 2.1. Materials

Western Jilin in China is the main carbonated saline soil distribution area, a representative seasonal frozen soil zone. Qian'an County is a representative distribution point of saline soil in this area. The saline soil in this area has significant dispersibility and is prone to damage under the action of water [43]. The average annual evaporation in this area is much larger than the annual average precipitation, which accelerates the formation of salinisation. Under the combined effect of infiltration and evaporation, the salt content is highest at a depth of 40 cm. Therefore, the experimental soil samples for this research were taken from a depth of 40 cm in Qian'an County. The original saline soil has a water content of 22.00%, a natural density of  $1.85 \text{ g/cm}^3$ , and a salt content of 0.51%. Table 1 reveals the basic physical properties, and Table 2 shows the chemical properties of the saline soil. Figure 1 shows the physical parameters of saline soil. From its physical property parameters, the saline soil here was classified as low liquid-limit clay (CL) on the basis of the Unified Soil Classification System (USCS) [45].

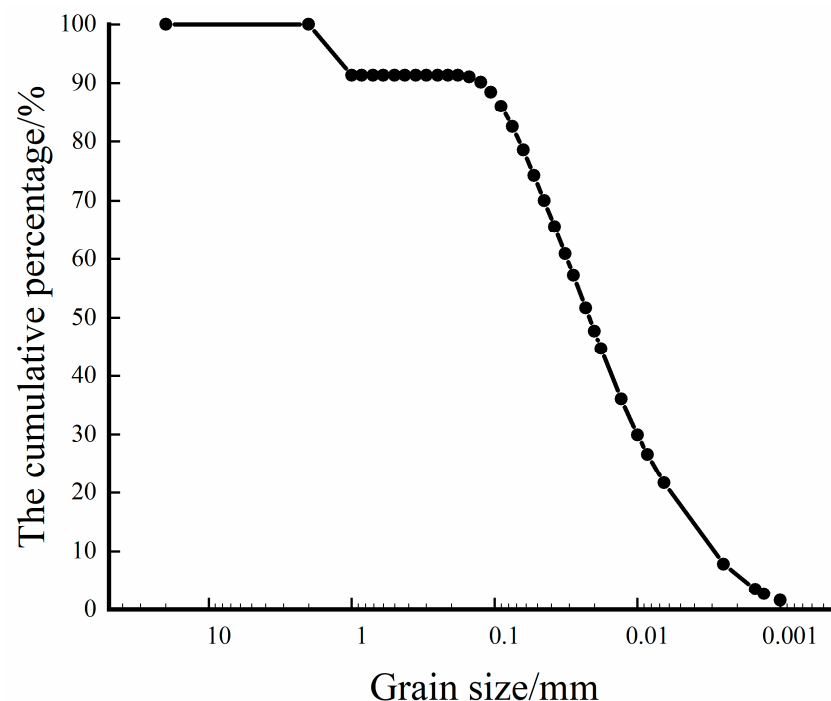


Figure 1. Grain size distribution curve.

**Table 1.** Basic physical properties.

Soil Type	Natural Density (g/cm <sup>3</sup> )	Natural Water Content (%)	Dry Density (g/cm <sup>3</sup> )	Specific Gravity of Solid Particles (g/cm <sup>3</sup> )	Plastic Limit (%)	Liquid Limit (%)	Plasticity Index	Liquidity Index
CL	1.85	22	1.78	2.71	17.1	36.66	19.56	0.25

**Table 2.** Basic chemical properties.

PH	Soluble Salt Content (%)	K <sup>+</sup> (mmol/kg)	Ca <sup>2+</sup> (mmol/kg)	Mg <sup>2+</sup> (mmol/kg)	Na <sup>+</sup> (mmol/kg)	SO <sub>4</sub> <sup>2-</sup> (mmol/kg)	CO <sub>3</sub> <sup>2-</sup> (mmol/kg)	HCO <sub>3</sub> <sup>-</sup> (mmol/kg)	Cl <sup>-</sup> (mmol/kg)
7.72	0.51	1.22	12.2	2.4	29.46	2.5	0	35.6	10.7

### 2.2. Specimen Preparation

The soil sample selected for this study was an in situ saline soil, so it was necessary to prepare the in situ standard triaxial specimens required for the experiment. The loss of water and the preservation method of the in situ soil samples can lead to changes in the structure of the in situ saline soil. Therefore, the in situ soil samples were stored in a moist environment, and the relevant tests were performed in time to avoid the loss of water and the disturbance of the in situ saline soil samples during the preservation process. For the preparation of in situ standard triaxial saline soil specimens, a soil cutter is required to prepare standard triaxial specimens of 39.1 mm in diameter and 80 mm in height. To prevent moisture loss from the in situ triaxial specimens, the prepared triaxial specimens were wrapped with cling film and stored in a moisturising cylinder. In order to reduce the disturbance to the in situ saline soil triaxial specimens, triaxial tests under different stress path conditions need to be performed in time.

### 2.3. Experimental Scheme

The drainage condition, consolidation method, stress path, and confining pressure were selected as the test variables, and a comprehensive test of the four factors was conducted. Two drainage conditions, drained and undrained, were selected; two consolidation methods, isobaric consolidation and  $K_0$  consolidation, were selected; the stress paths, conventional (constant confining pressure, increasing axial pressure), increased  $p$  (increasing confining pressure, increasing axial pressure, where the increase ratio  $\Delta\sigma_3/\Delta\sigma_1 = 0.5$ ), equal  $p$  (decreasing confining pressure, increasing axial pressure, constant mean total stress  $p$ ), and decreased  $p$  (decreasing confining pressure, constant axial pressure), were selected. Four stress paths and three stress levels of 100, 200, and 300 kPa were chosen for the confining pressure. Therefore, triaxial shear tests under six different conditions were conducted for the purpose of the study, including the consolidated undrained triaxial test under the conventional stress path under the isobaric consolidation condition (CU); the consolidated drained triaxial test under the conventional (CD), equal  $p$  (TC), reduced  $p$  (RTC), and increased  $p$  (CTC) stress paths under the isobaric consolidation condition; and the consolidated drained triaxial test under the conventional stress path under the  $K_0$  consolidation condition ( $K_0$ ). Table 3 shows the concrete experimental scheme of the test.

In order to achieve the research purpose of this test, the GDS unsaturated soil triaxial tester manufactured in the UK was selected for the triaxial shear test. Consolidation pressure was selected at three levels of 100, 200, and 300 kPa for a total of 18 groups of tests. The test steps are as follows: first, saturate the sample with a vacuum pumping in a saturator so the saturation can reach more than 95%, and then perform the consolidation process with a certain effective consolidation pressure; keep the consolidation pressure constant as the confining pressure after consolidation; finally, conduct triaxial shear experiments with different test conditions according to the above experimental scheme, and end the strain control to 16%.

**Table 3.** Experimental scheme of the test.

Triaxial Test Type	Experimental Conditions	Experiment Description	Confining Pressure (kPa)
Consolidated drained	Equal $p$ (TC)	Decrease in confining pressure, increase in axial pressure, constant mean total stress $p$ .	100, 200, 300
	Conventional (CD)	Constant confining pressure, increase in axial pressure, increase in mean total stress $p$ .	100, 200, 300
	Reduced $p$ (RTC)	Decrease in confining pressure, constant axial pressure, decrease in mean total stress $p$ .	100, 200, 300
	Increased $p$ (CTC)	Increase in confining pressure, increase in axial pressure ( $\Delta\sigma_3/\Delta\sigma_1 = 0.5$ ), increase in mean total stress $p$ .	100, 200, 300
	$K_0$ consolidation condition ( $K_0$ )	Conventional (CD) shear test under $K_0$ consolidation conditions.	100, 200, 300
Consolidated undrained	Conventional (CU)	Decrease in confining pressure, increase in axial pressure, constant mean total stress $p$ .	100, 200, 300

### 3. Results and Discussion

#### 3.1. Stress–Strain Relationship

Stress–strain relationships in soils are the basis of soil deformation and strength, and the evolution of pores and rearrangement of soil aggregates are strongly influenced by stress paths. This affects the stress–strain behaviour of the soil on a macroscopic scale and influences the interlocking forces between soil particles. Figure 2 shows the stress–strain relationship curves of in situ saline soils under different confining pressures under isobaric consolidation and  $K_0$  consolidation conditions. The following conclusions can be drawn from Figure 2: (1) Under the two consolidation conditions, the stress–strain relationship curve gradually shifts upward with the increase in the confining pressure, and the shear strength of the specimen gradually increases, indicating that the confining pressure increases the shear strength of the soil by improving the compressive rigidity of the saline soil. (2) Regarding the degree of strain hardening, under different confining pressures, the degree of strain hardening under isobaric consolidation conditions is stronger than that under  $K_0$  consolidation conditions, which is due to the fact that  $K_0$  consolidation conditions can maintain the structural properties of the specimens better than isobaric consolidation conditions, and their compaction effect is weaker, so the degree of strain hardening is weaker. (3) Comparing the relative positions of the curves under the two consolidation conditions, the deviatoric stress  $q$  values under the isobaric consolidation condition are smaller than those under the  $K_0$  consolidation condition in the early stage of axial strain under different confining pressures because the structural properties of the specimens under the  $K_0$  consolidation conditions are stronger than those under the isobaric consolidation conditions. With the development of axial strain, the values of deviatoric stress  $q$  at the destruction of the specimens under isobaric consolidation are larger than those under  $K_0$  consolidation, which indicates that the shear strength of the soil is increased under isobaric consolidation compared with  $K_0$  consolidation.

The relationship curve of deviatoric stress  $q$ –axial strain  $\epsilon_1$  for in situ saline soils under different confining pressures with different drainage conditions is shown in Figure 3. From the figure, it can be seen that the stress–strain curves for the consolidated drained conditions are all located above the stress–strain curves for the consolidated undrained conditions under the same confining pressure, indicating that the shear strength under the drained conditions is greater than that under the undrained conditions. This difference is related to

whether the soil is drained during the shear stage, which occurs as a result of the draining process in the shear stage, which makes the water content in the soil lower. Additionally, the specimen becomes denser during the shear stage, and the occlusion between soil particles is enhanced, which leads to an increase in friction, so the shear strength increases. On the other hand, because the test soil sample is saline soil, the presence of salt in the soil makes the double electric layer thinner and more structural under the reduced water content, resulting in the shear strength of the specimen under the drained conditions being greater than that of the specimen under the undrained conditions.

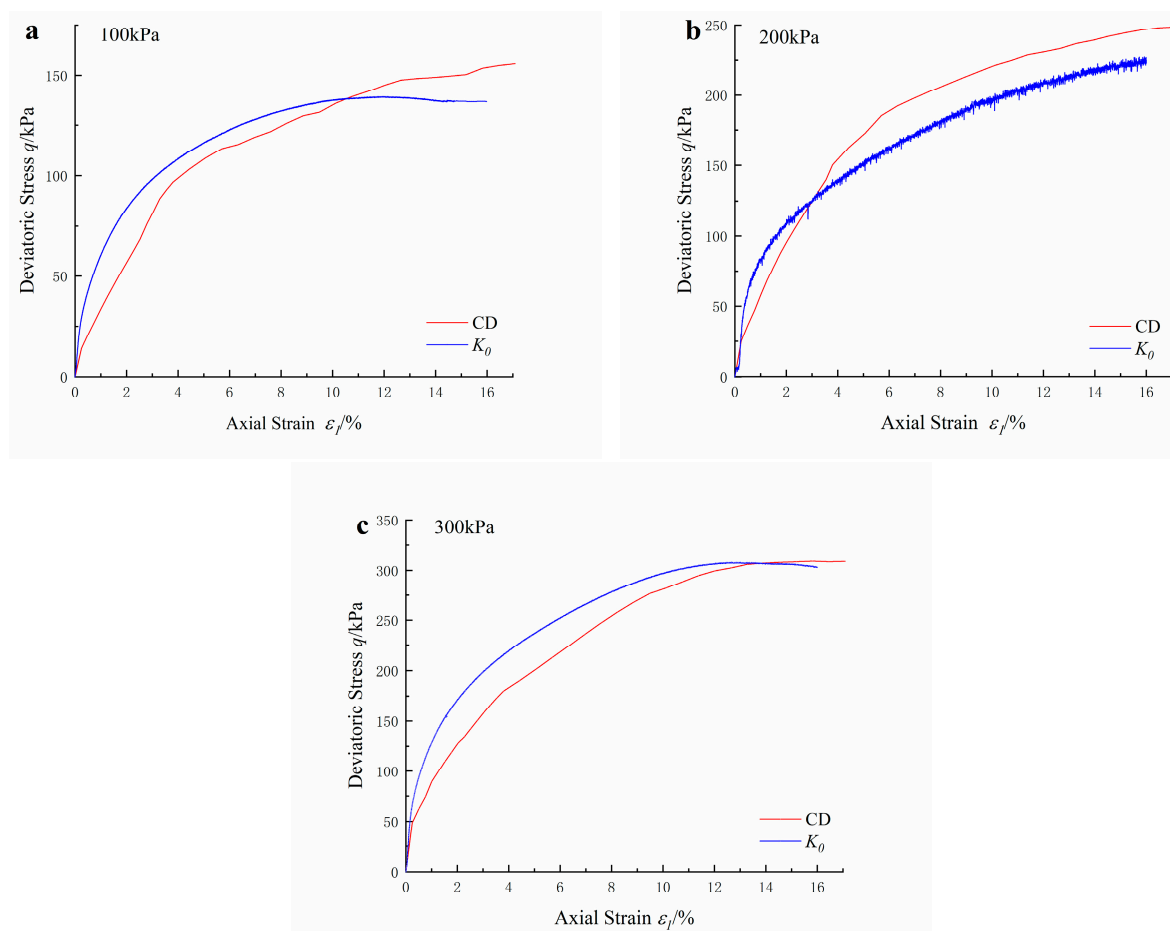


**Figure 2.** Deviatoric stress  $q$ –axial strain  $\varepsilon_1$  relationship curve under different consolidation conditions. (a) 100 kPa. (b) 200 kPa. (c) 300 kPa.

The relationship curve of deviatoric stress  $q$ –axial strain  $\varepsilon_1$  for in situ saline soils under the four different stress paths of conventional (CD), equal  $p$  (TC), reduced  $p$  (RTC), and increased  $p$  (CTC) are shown in Figure 4. It can be seen from the figure that the stress–strain relationship curves of the soil under the same confining pressure increase sequentially in the order of reduced  $p$  (RTC), equal  $p$  (TC), conventional (CD), and increased  $p$  (CTC). With the development of axial strain, the stress–strain relationship curve tends to level off the earliest under the reduced  $p$  (RTC) stress path, and then the stress paths under equal  $p$  (TC), conventional (CD), and increased  $p$  (CTC), in that order. When the deformation of the specimen develops into damage, the relationship between the magnitude of the shear strength under the four different stress paths is increased in the order of  $p$  (CTC) > conventional (CD) > equal  $p$  (TC) > reduced  $p$  (RTC). After isobaric consolidation, the stress–strain relationship curves under different stress paths showed strain-hardening characteristics, and the strain-hardening degree gradually decreased in the order of increased  $p$  (CTC), conventional (CD), equal  $p$  (TC), and reduced  $p$  (RTC), which was related to the size of the confining pressure at the end of the shear stage.

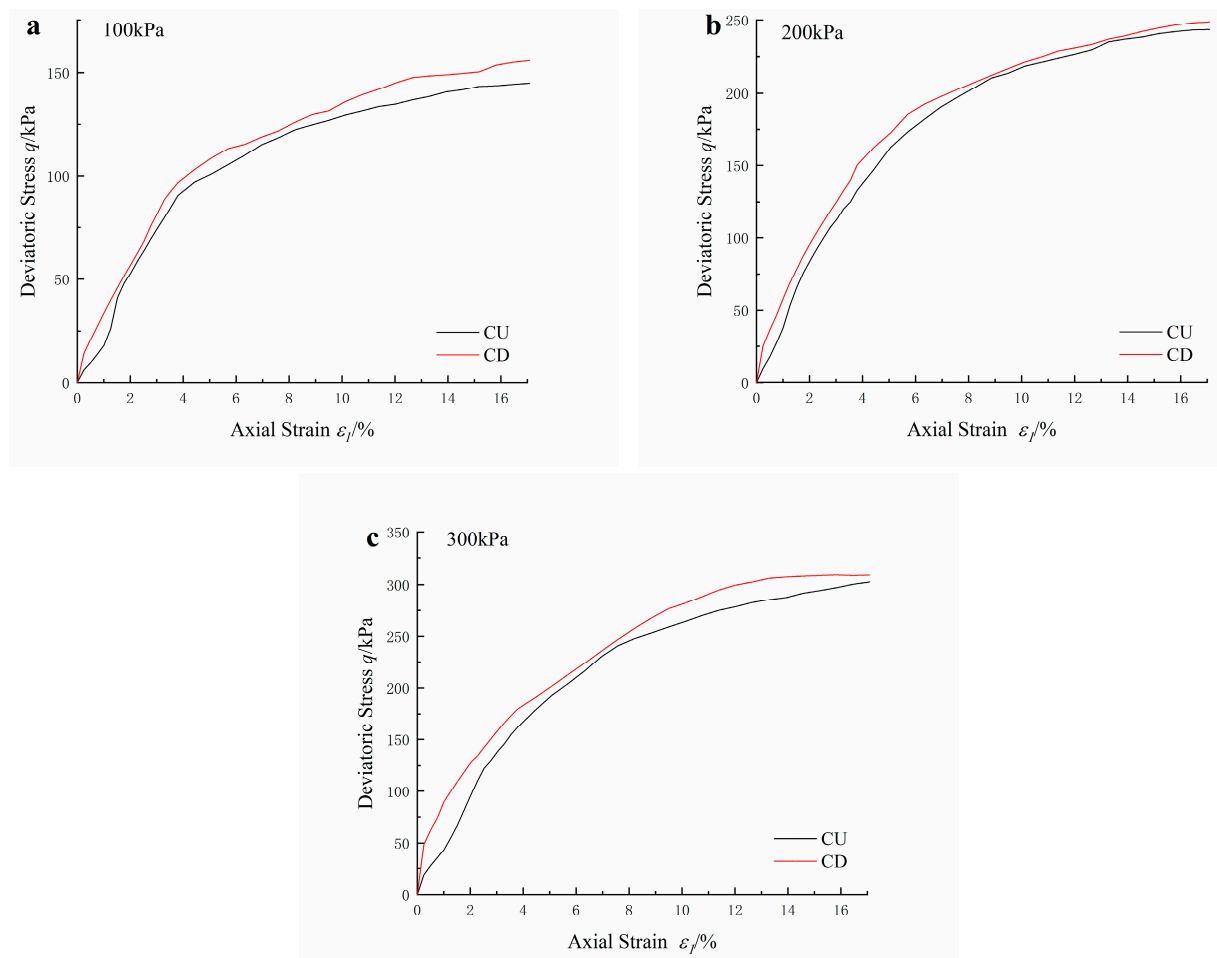


**Figure 3.** Deviatoric stress  $q$ –axial strain  $\epsilon_1$  relationship curve under different drainage conditions. (a) 100 kPa. (b) 200 kPa. (c) 300 kPa.

Soil deformations occur under different stress paths, among which, the soil can be compressed and dense under the action of spherical stress  $p$ , thus producing a constraint effect. The spherical stress  $p$  decreases continuously in the order of increased  $p$  (CTC), conventional (CD), equal  $p$  (TC), and reduced  $p$  (RTC). Under the reduced  $p$  (RTC) stress path, the constraint effect of the soil gradually decreases with the decreasing spherical stress  $p$ , and plastic deformation is produced under lower axial-strain conditions. Therefore, the reduced  $p$  (RTC) stress–strain curve enters a flat state the earliest. Comparing the four different stress paths, the confining pressure decreases under the reduced  $p$  (RTC) and equal  $p$  (TC) stress paths, the constraint effect gradually decreases, the interparticle friction decreases, and a lower deviatoric stress is required to produce the corresponding deformation; the confining pressure remains unchanged under the conventional (CD) stress path; and the confining pressure increases under the increased  $p$  (CTC) stress path, the constraint effect increases, the interparticle friction increases, and higher deviatoric stress is required to produce the corresponding deformation, so the shear strength of the specimen is larger. Under the same confining pressure, as the magnitude relationship of spherical stress  $p$  increases in the order of  $p$  (CTC) > conventional (CD) > equal  $p$  (TC) > reduced  $p$  (RTC), its constraint effect weakens, and the compaction effect also weakens, which leads to the strain-hardening characteristic of the stress–strain curve also weakening.

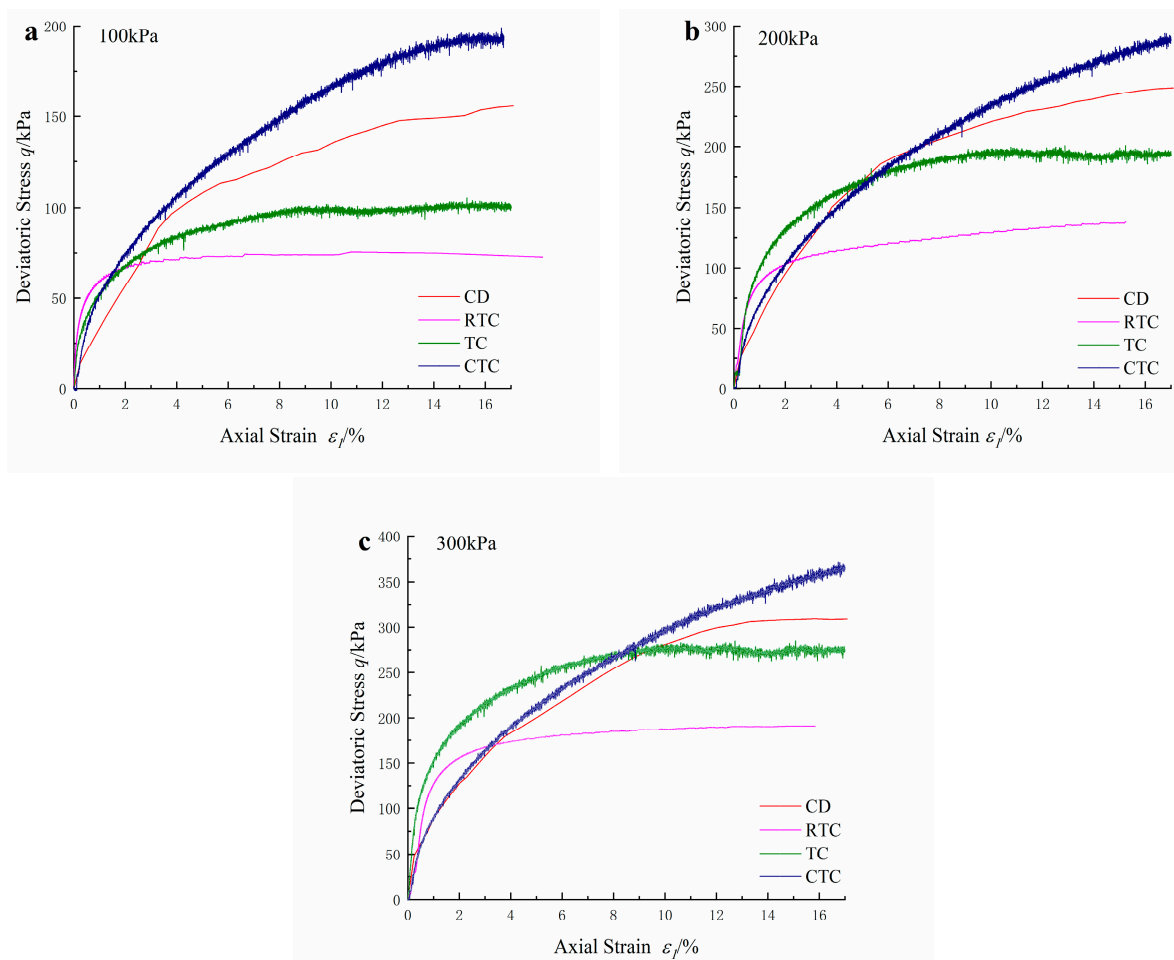


**Figure 4.** Deviatoric stress  $q$ –axial strain  $\varepsilon_1$  relationship curve under different stress paths. (a) 100 kPa. (b) 200 kPa. (c) 300 kPa.

### 3.2. Stress Path

Because the triaxial tests under the five different test conditions of conventional (CD), equal  $p$  (TC), reduced  $p$  (RTC), increased  $p$  (CTC), and  $K_0$  in this test all used the test method of consolidation and draining, for this test method, because it is necessary to maintain the pore water pressure at 0 at all times during the experiment, resulting in two stress paths of total stress and effective stress that are the same, in order to facilitate the analysis, the total stress path was chosen for the analysis of the stress path under the consolidated undrained conditions (CU).

The relationship between the stress path curve and the stress path of the specimen under different confining pressure conditions is shown in Figure 5. From the figure, it can be seen that the change characteristics of the curves under different stress paths under the same confining pressure show obvious differences, but the initial positions are the same from left to right for the stress path curves under the conventional (CD), equal  $p$  (TC), reduced  $p$  (RTC), and increased  $p$  (CTC) stress paths.

- (1) Under the conventional stress path, the stress paths under the consolidated undrained (CU), consolidated drained (CD), and  $K_0$  consolidated ( $K_0$ ) triaxial test conditions appear to overlap, and the three are similar, and the stress path curves show a linear increasing trend because the confining pressure  $\sigma_3$  remains constant and the axial pressure gradually increases under this stress path, and the slope of the stress path curve is calculated to be 1 because  $\Delta\sigma_3 = 0$ .
- (2) For the equal  $p$  (TC) stress path, because the confining pressure is the same in the triaxial shear test, i.e.,  $\sigma_2 = \sigma_3$ , the spherical stress  $p = (\sigma_1 + \sigma_2 + \sigma_3)/3$  of the soil

sample remains constant under the equal  $p$  (TC) stress path condition, i.e.,  $(\sigma_1 + 2\sigma_3)/3$  remains constant, so that  $\Delta\sigma_1 = -2\Delta\sigma_3$ , and the slope of the stress path curve can be calculated to be 3.

- (3) For the reduced  $p$  (RTC) stress path, the axial pressure remains unchanged, i.e.,  $\Delta\sigma_1 = 0$ , and the confining pressure decreases, and the slope of the stress path curve can be calculated as  $-1$ .
- (4) For the increased  $p$  (CTC) stress path,  $\sigma_3$  increases and  $\sigma_1$  increases, and the ratio of both increases is  $\Delta\sigma_3/\Delta\sigma_1 = 0.5$ . In the triaxial test,  $\sigma_2 = \sigma_3$ ; therefore,  $\Delta\sigma_1 = 2\Delta\sigma_3$ , and the slope of the stress path curve can be calculated as  $1/3$ .

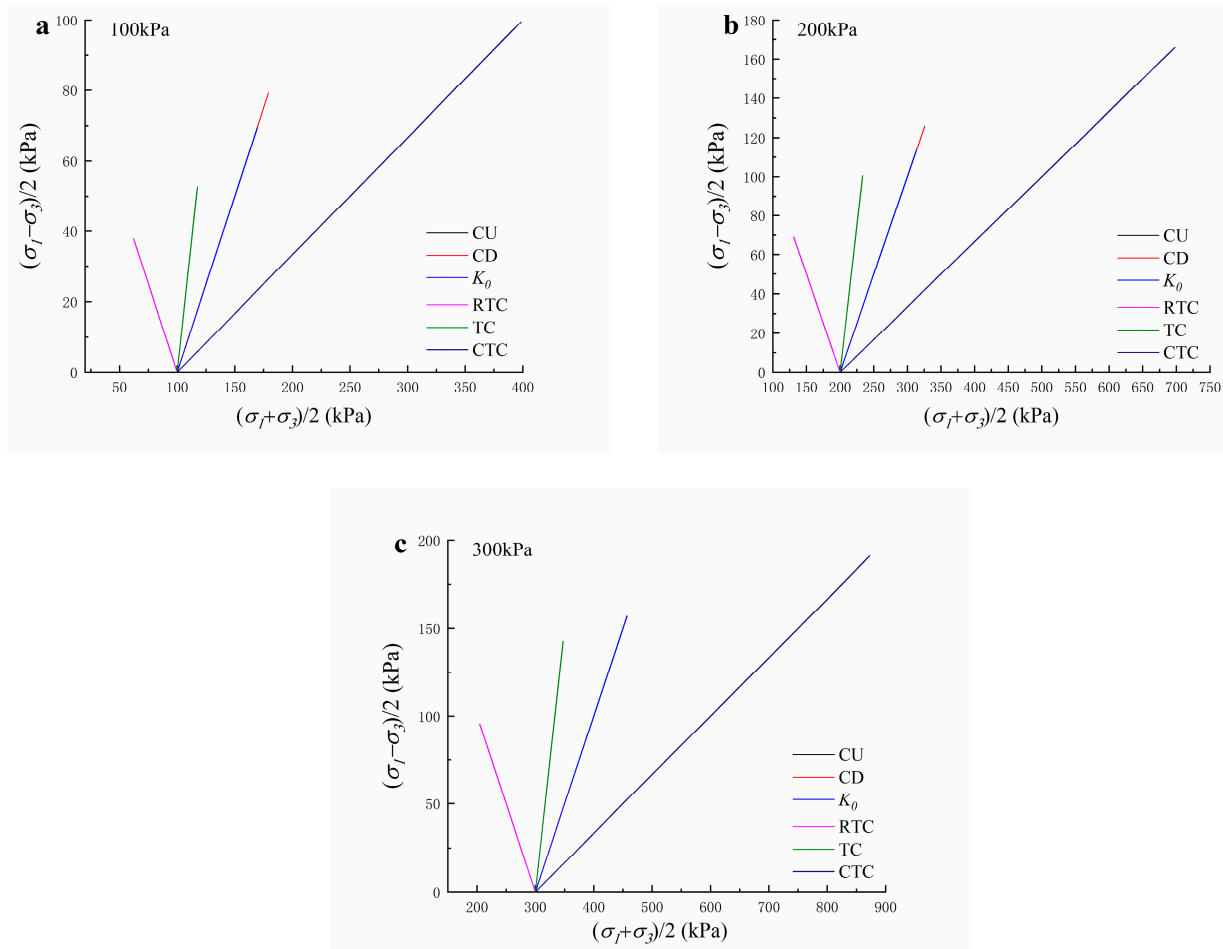


**Figure 5.** Total stress path curves under different stress paths. (a) 100 kPa. (b) 200 kPa. (c) 300 kPa.

Under different stress path conditions, the stress path curve of the specimen varies with the confining pressure as shown in Figure 6. It can be seen that under the same stress path, the slopes of the stress path curves of the in situ saline soils are the same, and they show parallel characteristics under different confining pressures, and different confining pressures only have different relative positions on the curves. Under the confining pressures of 100 kPa, 200 kPa, and 300 kPa, the  $p$  values at the starting points of the stress path curves under the different paths are 100 kPa, 200 kPa, and 300 kPa, indicating that the initial confining pressure value is the starting value of the stress path curves, and there are no obvious inflection points on the stress path curves under the four stress paths of conventional (CD), equal  $p$  (TC), reduced  $p$  (RTC), and increased  $p$  (CTC).

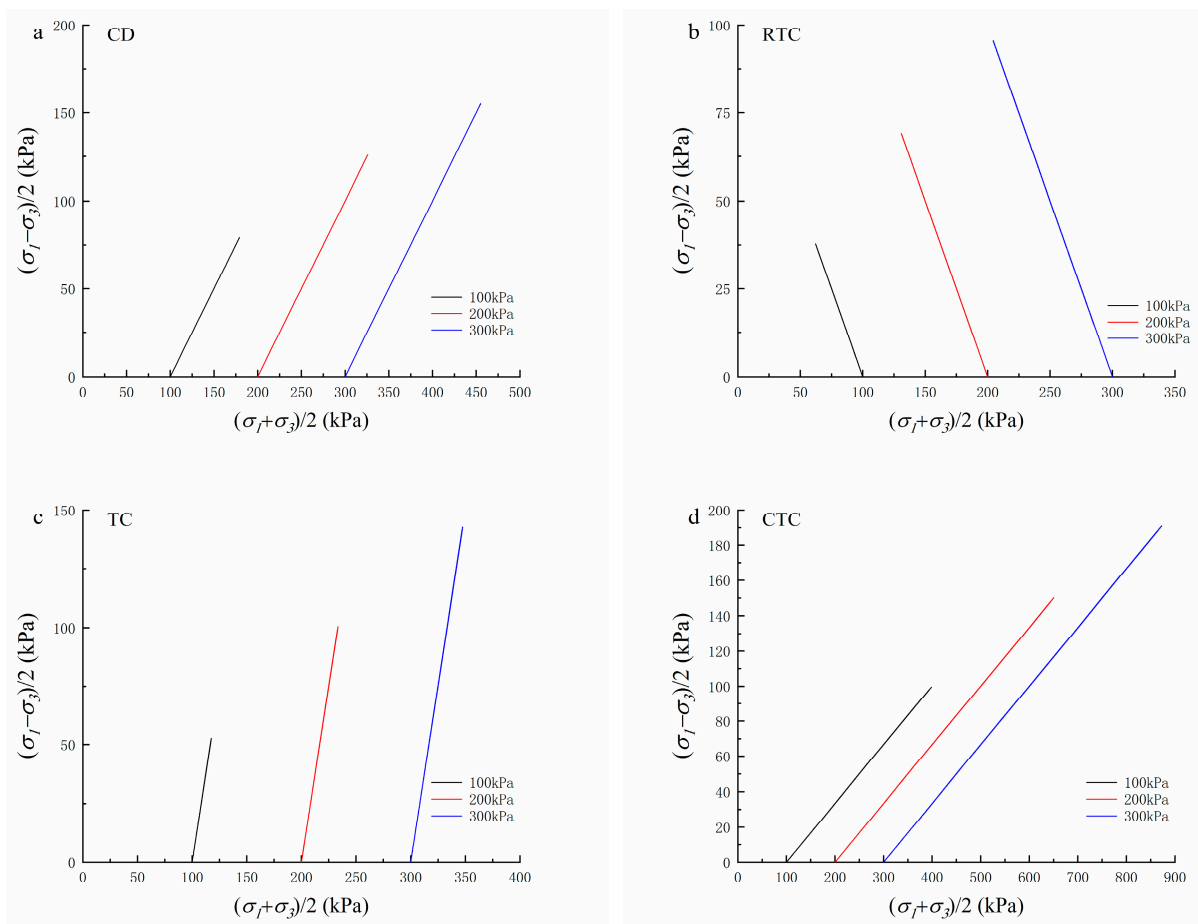


Figure 6. Total stress path curves under different confining pressures. (a) CD. (b) RTC. (c) TC. (d) CTC.

### 3.3. Shear Strength

According to the specification standard, the shear strength is taken as follows: when the stress–strain relationship curve of the specimen is strain-hardened, the deviatoric stress value at 15% of the axial strain is taken as the shear strength value of the specimen. In order to better represent the shear strength variation of the specimen, it is shown in Figure 7.

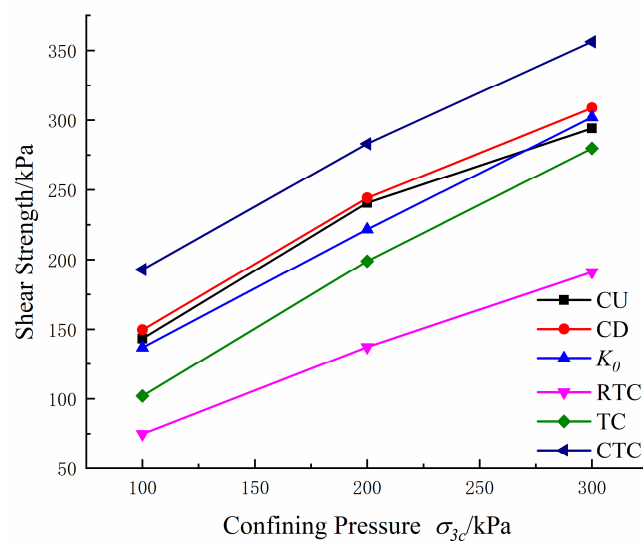


Figure 7. Variation in shear strength under different stress paths.

Under the same path, the shear strength of the soil gradually increases with the increase in the confining pressure, which is consistent with universal research law, because the gaps between soil particles decrease under the confining pressure, which makes the friction between soil particles increase, and the soil becomes more compact. Saline soil is a special soil because of the presence of salt in the soil, and under conditions of higher confining pressure, the drainage increases and the water content is relatively low as a result of the thinning of the double electric layer caused by the salt. Additionally, the force between soil particles is enhanced, which makes the confining pressure have an enhanced effect on the shear strength such that greater force is required when damage to the specimen occurs; thus, the shear strength of the soil sample is continuously enhanced with the increase in the confining pressure.

For the same initial confining pressure, the shear-strength magnitude relationships of saline soils under different stress paths are shown as follows: increased  $p$  (CTC) > conventional (CD) > equal  $p$  (TC) > reduced  $p$  (RTC). This can also be explained by examining the effect of the above confining pressure on specimen strength. Comparing the changes in spherical stress  $p$  under the different stress paths, the spherical stress  $p$  increases and the confining pressure  $\sigma_{3c}$  increases under the increased  $p$  (CTC) stress path; under the conventional (CD) stress path, the spherical stress  $p$  increases and the confining pressure  $\sigma_{3c}$  remains unchanged; under the equal  $p$  (TC) stress path, the spherical stress  $p$  remains unchanged and the confining pressure  $\sigma_{3c}$  decreases; and under the reduced  $p$  (RTC) stress path, the spherical stress  $p$  decreases and the confining pressure  $\sigma_{3c}$  decreases, which leads to the magnitude of shear strength under the different stress paths showing the following order: increased  $p$  (CTC) > conventional (CD) > equal  $p$  (TC) > reduced  $p$  (RTC). In addition, the increasing spherical stress  $p$  leads to more drainage in the shear stage, which leads to the thinning of the double electric layer caused by salt in the saline soils, making the bonding force stronger and leading to the increase in shear strength.

#### 4. Shear Strength Parameters

Among the strength theories of soil, the Mohr–Coulomb strength theory is the most widely used, which uses the two indicators of cohesion ( $c$ ) and internal friction angle ( $\varphi$ ) to express shear strength. The shear strength parameters of soil are widely used in geotechnical engineering design, and there are differences in the shear strength of soil under different stress paths; therefore, it is of great practical engineering importance to study the shear strength parameters of soil under different stress paths. Under different stress paths, the Mohr–Coulomb strength criterion is still applicable, so this section finds out the shear strength values of soils under different stress path conditions according to the corresponding codes and plots of the Mohr–Coulomb strength envelopes for in situ saline soils under different stress paths.

The stress path method is used to solve the shear strength parameters under different stress path conditions. For the equal  $p$  (TC), reduced  $p$  (RTC), and increased  $p$  (CTC) stress paths,  $\sigma_3$  and  $\sigma_1$  are loaded according to the test design criteria, and  $\sigma_{3f}$  and  $\sigma_{1f}$  at the time of specimen damage are used in the Mohr circle plotting.

The values of cohesion  $c$  and internal friction angle  $\varphi$  in different conditions were obtained from the stress Molar circles plotted under different conditions according to the triaxial test data, as shown in Figure 8 below.

According to Figure 8 above, the shear strength parameters under different conditions, cohesion  $c$  and internal friction angle  $\varphi$ , are obtained, and the specific results are shown in Table 4 below.

**Table 4.** Cohesion  $c$  and internal friction angle  $\varphi$  under different conditions.

Shear Strength Parameters	CU	CD	$K_0$	RTC	TC	CTC
$c$ (kPa)	27.93	27.78	20.32	14.24	7.50	25.36
$\varphi$ (°)	15.98	16.57	17.00	24.08	22.76	10.63

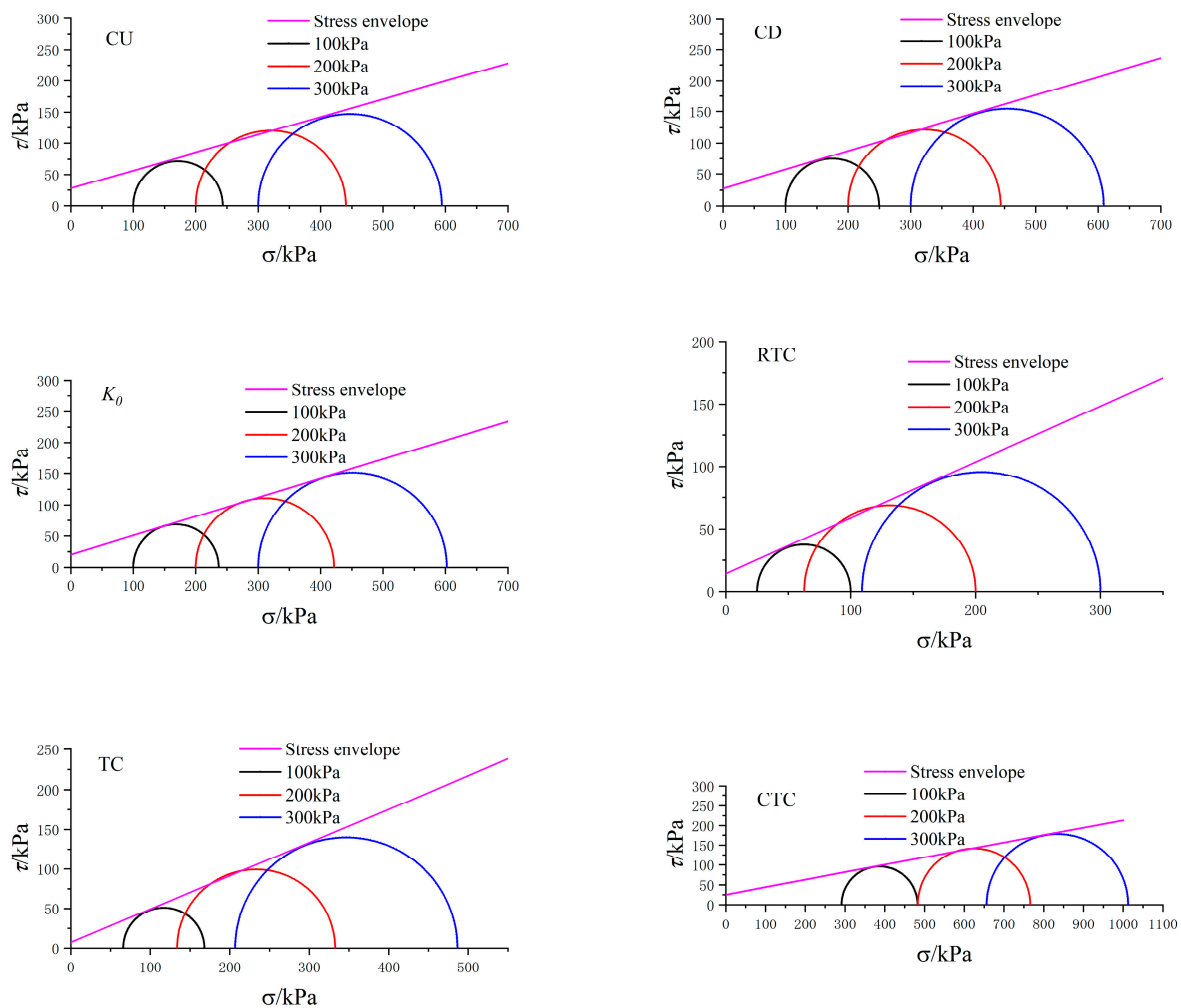


Figure 8. Stress Mohr circle under different conditions.

From Table 4, it can be seen that (1) comparing the shear strength parameters under the two conditions of undrained and drained, the drainage condition has a smaller effect on the cohesion  $c$  and a larger effect on the internal friction angle  $\varphi$  during the shear process, where the internal friction angle  $\varphi$  is larger under the drained conditions than under the undrained conditions; (2) comparing the shear strength parameters under the two conditions of isobaric consolidation and  $K_0$  consolidation, the effect of the consolidation condition on the cohesion  $c$  is larger and the effect on the internal friction angle  $\varphi$  is smaller, and the cohesion  $c$  under the  $K_0$  consolidation condition is smaller than that under the isobaric consolidation condition; and (3) comparing the shear strength parameters under the four different stress path conditions of conventional (CD), equal  $p$  (TC), reduced  $p$  (RTC), and increased  $p$  (CTC), after isobaric consolidation, the stress paths have a greater effect on both cohesion  $c$  and internal friction angle  $\varphi$  during the drained shear stage.

Regarding the shear strength parameters of in situ saline soils under different drainage conditions, the drainage condition has a greater effect on the value of internal friction angle  $\varphi$  and a smaller effect on the value of cohesion  $c$  because of the draining effect during the shear stage, which makes the water between soil particles drain, and the water between particles has a certain lubricating effect; with the occurrence of drainage, the lubricating effect is weakened and the friction effect is enhanced, resulting in the value of internal friction angle  $\varphi$  under the drained conditions being larger than the internal friction angle  $\varphi$  under the undrained conditions.

Regarding the shear strength parameters of in situ saline soils under different initial consolidation conditions, the effect of the initial consolidation condition on cohesion  $c$

is larger, and the effect on the value of internal friction angle  $\varphi$  is smaller. Regarding the comparison of shear strength under two the conditions of isobaric consolidation and  $K_0$  consolidation, the strength under isobaric consolidation is greater than that under  $K_0$  consolidation, so the values of cohesion  $c$  obtained from isobaric consolidation are also greater than the values of cohesion  $c$  under  $K_0$  consolidation, indicating that the difference in shear strength mainly comes from the difference in cohesion  $c$ .

As a special soil, saline soil is also a cohesive soil, and the mineral particles are mostly flat in shape, forming different binding water in different parts and thus making the saline soil show certain anisotropy. The binding water is different from gravitational water, which is more strongly combined with soil particles and can influence and transfer the force between particles. This effect is made more obvious by the presence of a variety of soluble salt components in saline soil soils, and the corresponding soil structure is changed. As a result of the presence of salts, the double electric layer thickens and various electrochemical forces as well as the occlusion between particles are reduced, which leads to a decrease in the strength of saline soils and makes them more affected by the change in stress state.

In general, for the value of cohesion  $c$ , the cohesion  $c$  under the equal  $p$  (TC) stress path is the smallest, and the cohesion  $c$  under the reduced  $p$  (RTC) and increased  $p$  (CTC) stress path conditions increases sequentially, and the cohesion  $c$  under the conventional (CD) stress path is the largest. For the value of the internal friction angle  $\varphi$ , the internal friction angle  $\varphi$  is the largest under the reduced  $p$  (RTC) stress path and decreases under the equal  $p$  (TC), conventional (CD), and increased  $p$  (CTC) stress paths because spherical stress  $p$  is decreasing under the reduced  $p$  (RTC) stress path, but the axial pressure remains unchanged, resulting in radial expansion of the soil, and this process makes the energy absorbed by the soil particle friction increase, thus maximising the value of internal friction angle  $\varphi$  under the reduced  $p$  (RTC) stress path.

## 5. Conclusions

In this paper, the mechanical properties of Qian'an saline soils under different stress path conditions were investigated. Standard triaxial specimens of in situ saline soils were prepared in a laboratory, and then triaxial shear tests were conducted under six different stress path conditions. The mechanical properties of the saline soils under different stress path conditions were investigated, and the specific conclusions are as follows:

- (1) Regarding stress–strain relationships: The stress–strain relationships of the specimens all showed strain-hardening characteristics. Regarding the stress–strain relationship curves when the specimens were damaged, those under  $K_0$  consolidation conditions were all located above those under the isobaric consolidation conditions. The stress–strain curves under the drained conditions are all located above those of the undrained conditions. The stress–strain curves of the soil under the different stress path conditions are shifted upward in the following order: reduced  $p$  (RTC), equal  $p$  (TC), conventional (CD), and increased  $p$  (CTC).
- (2) Regarding stress path characteristics: The stress path curves under the same stress path have the same slope and do not have obvious inflection points. Under the conventional stress path, the slope is 1; under the increased  $p$  stress path, the slope is 1/3; under the equal  $p$  stress path, the slope is 3; under the decreased  $p$  stress path, the slope of the curve is  $-1$ . For different confining pressures, only the relative positions of the curves are different. Under the same consolidation pressure, the left to right order is as follows: reduced  $p$  (RTC), equal  $p$  (TC), conventional (CD), and increased  $p$  (CTC).
- (3) Regarding shear strength: Under the same confining pressure, the relationship between the magnitude of the shear strength of saline soil under different stress paths is expressed in the following order: increased  $p$  (CTC) > conventional (CD) > equal  $p$  (TC) > reduced  $p$  (RTC).
- (4) Regarding shear strength parameters: In the shear stage, the drainage condition has a smaller effect on the cohesion  $c$  and a larger effect on the internal friction angle  $\varphi$ ;

the consolidation condition has a greater effect on the cohesion  $c$  and a smaller effect on the internal friction angle  $\varphi$ ; and the stress paths have a greater effect on both cohesion  $c$  and internal friction angle  $\varphi$ .

**Author Contributions:** Conceptualisation, S.C. and Q.W.; methodology, S.C.; software, Y.H.; validation, S.C.; formal analysis, S.C.; investigation, J.W.; resources, Q.W.; data curation, S.C.; writing—original draft preparation, S.C.; writing—review and editing, S.C.; visualisation, S.C.; supervision, Q.W.; project administration, Q.W.; funding acquisition, Q.W. All authors have read and agreed to the published version of the manuscript.

**Funding:** This work was supported by the Key Program of International (Regional) Cooperation and Exchange of National Natural Science Foundation (Grant No. 41820104001), State Key Program of the National Natural Science Foundation of China (Grant No. 41430642), and the Special Fund for Major Scientific Instruments of the National Natural Science Foundation of China (Grant No. 41627801).

**Data Availability Statement:** The data presented in this study are available on request from the corresponding author.

**Acknowledgments:** We sincerely thank all the reviewers and editors for their professional comments and suggestions regarding this manuscript.

**Conflicts of Interest:** The authors declare no conflict of interest.

## References

- Chen, C.; Guo, J.; Yang, P. Influence of stress path on deformation and strength characteristics of saturated intact loess under drainage condition. *J. Hydraul. Eng.* **2008**, *39*, 6.
- Li, Z. Test Study on Engineering Characteristics of Lime-improved Saline Soil for Highway Subgrade. *J. Shijiazhuang Railw. Inst.* **2007**, *2*, 45–48+114.
- Wu, A.; Cai, L.; Gu, Q.; Wang, Z. Ground Treatment of Airport by Heavy Cover Technique in Sulphate Saline Soil Region. In Proceedings of the International Conference on Transportation Engineering, Chengdu, China, 25–27 July 2009.
- Wang, W.W.; Yang, B.C.; Wang, R. Road diseases in southern saline soil areas of Xinjiang. *Chin. J. Geotech. Eng.* **2013**, *35*, 253–258.
- Cheng, S.; Wang, Q.; Fu, H.; Wang, J.; Han, Y.; Shen, J.; Lin, S. Effect of freeze-thaw cycles on the mechanical properties and constitutive model of saline soil. *Geomech. Eng.* **2021**, *27*, 309–322.
- Lai, Y.M.; You, Z.M.; Zhang, J. Constitutive models and salt migration mechanisms of saline frozen soil and the-state-of-the-practice countermeasures in cold regions. *Sci. Cold Arid Reg.* **2021**, *13*, 1–17.
- Li, X.; Guo, L.; Cai, Y.; Hu, X. Stress path triaxial tests on K0-consolidated saturated soft clay. *Zhongnan Daxue Xuebao (Ziran Kexue Ban)/J. Cent. South Univ. (Sci. Technol.)* **2015**, *46*, 1820–1825.
- Zhuang, H.; Wang, J.; Gao, Z. Anisotropic and Noncoaxial Behavior of Soft Marine Clay under Stress Path Considering the Variation of Principal Stress Direction. *Int. J. Geomech.* **2022**, *22*, 04022062. [[CrossRef](#)]
- Pan, K.; Yang, Z.X.; Cai, Y.Q. Flow liquefaction potential of loose sand: Stress path envelope and energy-based evaluation. *Can. Geotech. J.* **2021**, *58*, 1783–1789. [[CrossRef](#)]
- Shi, C.; Yang, J.; Chu, W.; Tang, H.; Zhang, Y. Macro- and Micromechanical Behaviors and Energy Variation of Sandstone under Different Unloading Stress Paths with DEM. *Int. J. Geomech.* **2021**, *21*, 04021127. [[CrossRef](#)]
- Kandasami, R.K.; Murthy, T.G.; Singh, S. Experimental Investigations of the Stress Path Dependence of Weakly Cemented Sand. *J. Geotech. Geoenviron. Eng.* **2021**, *147*, 04021007. [[CrossRef](#)]
- Cai, Y.; Hao, B.; Gu, C.; Wang, J.; Pan, L. Effect of anisotropic consolidation stress paths on the undrained shear behavior of reconstituted Wenzhou clay. *Eng. Geol.* **2018**, *242*, 23–33. [[CrossRef](#)]
- Lambe, T.W. Stress Path Method. *J. Soil Mech. Found. Div.* **1967**, *93*, 1195–1217.
- Liu, E.; Shen, Z. Mechanical Behavior of Structured Soils under Different Stress Paths. *Chin. J. Rock Mech. Eng.* **2006**, *25*, 7.
- Zeng, L.; Chen, X. Analysis of mechanical characteristics of soft soil under different stress paths. *Rock Soil Mech.* **2009**, *30*, 1264–1270.
- Gao, B.; Chen, J.; Yang, H.; Cheng, X.; Wu, Z. Experimental Study on Mechanical Properties of Red Clay under Different Stress Paths. *Chin. J. Undergr. Space Eng.* **2018**, *14*, 11.
- Lade, P.V.; Duncan, J.M. Stress-path dependent behavior of cohesionless soil. *J. Geotech. Eng. Div.* **1976**, *102*, 51–68. [[CrossRef](#)]
- Santos, O.F., Jr.; Lacerda, W.A.; Ehrlich, M. Collapse of saturated soil due to reduction in confinement. *J. Geotech. Eng.* **1996**, *122*, 505. [[CrossRef](#)]
- Sun, Y.; Pu, J.; Li, G. Effect of different stress paths on stress-strain relationships in sandy soils. *Chin. J. Geotech. Eng.* **1987**, *6*, 78–88.
- Breth, H.; Schuster, E.; Pise, P. Axial Stress-Strain Characteristics of Sand. *ASCE Soil Mech. Found. Div. J.* **1973**, *99*, 617–632. [[CrossRef](#)]

21. Xu, C.S.; Wen, L.M.; Du, X.L.; Xu, H.B. Experimental study on shear behaviors of sand under different stress path. *J. Hydraul. Eng.* **2010**, *41*, 108–112.
22. Silvestri, V.; Diab, R. Stress distributions and paths in clays during pressuremeter tests. *Can. Geotech. J.* **2001**, *38*, 542–552. [[CrossRef](#)]
23. Chang, Y.; Wang, X.; Zai, J.; Xu, J. Stress path test of cohesive soils. *J. Nanjing Tech Univ. (Nat. Sci. Ed.)* **2005**, *27*, 9–14.
24. Liu, Y.; Shi, J.; Yi, Y.; Xo, L. Experimental study of mechanical characteristics of an incomplete consolidation silty clay. *Rock Soil Mech.* **2004**, *25*, 5.
25. Kong, L.; Zang, M.; Guo, A.; Tuo, Y. Stress path effects on strength characteristics of Zhanjiang strong structural clay. *Rock Soil Mech.* **2015**, *36* (Suppl. S1), 19–24.
26. Wang, X.; Chen, F.; Cai, Y. Research on characteristics of shear deformation of silty clay in different stress paths. *Tunn. Constr.* **2011**, *31*, 192–196.
27. Huang, Y.; Liu, G.; Qi, L.; Tao, H.; Zheng, R.; Gu, Q. Experimental study of stress paths of saturated soft clay soils under different temperatures. *Hydrogeol. Eng. Geol.* **2016**, *43*, 5.
28. Shi, J.; Liu, Z. The effect of stress path on stress-strain relationship of loess. *J. Archit. Civ. Eng.* **1992**, *1*, 10–14.
29. Liang, Y.; Xie, Y.; Liu, H.C. Influence of stress path on consolidated undrained shear strength of loess. *Rock Soil Mech.* **2007**, *28*, 364–366.
30. Jiang, M.; Hu, H.; Peng, J.; Yang, Q. Pore changes of loess before and after stress path tests and their links with mechanical behaviors. *Chin. J. Geotech. Eng.* **2012**, *34*, 1369–1378.
31. Hu, H.; Jiang, M.; Peng, J.; Shen, Z. Pore fractal features of different kind of loesses before and after stress path test. *Rock Soil Mech.* **2014**, *35*, 7.
32. Hou, X.; Li, T.; Li, P. Analysis of stress path and deformation-failure mechanism of high cutting loess slope. *Rock Soil Mech.* **2014**, *35*, 548–555.
33. Zhao, D.; Fu, Y.K.; Hou, X.; Li, T.; Li, P.; Li, Y.; Zhang, L. Mechanical properties of saturated remolded loess under different stress paths. *Hydrogeol. Eng. Geol.* **2022**, *46*, 74–80.
34. Lo, S.; Lee, I.K. Response of Granular Soil along Constant Stress Increment Ratio Path. *J. Geotech. Eng.* **1990**, *116*, 32012.
35. Chen, C.; Hu, Z.; Wang, Z. The influence of stress paths on the stress-strain relationship of reinforced soil. *Power Syst. Clean Energy* **1998**, *1*, 13–16.
36. Hu, D.; Gao, Z.; Zhang, Q. Study on Constitutive Model of Fly Ash under Different Stress Paths. *J. Hydraul. Eng.* **1998**, *4*, 20–26.
37. Xiang, B.; Zhang, Z.L.; Chi, S.C. An improved hypoplastic constitutive model of rockfill considering effect of stress path. *J. Cent. South Univ. Technol. (Engl. Ed.)* **2009**, *16*, 1006–1013. [[CrossRef](#)]
38. Guo, Z.; Shi, X. *Temperature–Stress Paths and Coupling Constitutive Relation of Concrete*; Elsevier Inc.: Amsterdam, The Netherlands, 2011.
39. Nguyen, V.H.; Gland, N.; Dautriat, J.; David, C.; Wassermann, J.; Guélard, J. Compaction, permeability evolution and stress path effects in unconsolidated sand and weakly consolidated sandstone. *Int. J. Rock Mech. Min. Sci.* **2014**, *67*, 226–239. [[CrossRef](#)]
40. Zhang, J.; Luo, X.; Pang, W.K.; Zhang, B. Drained triaxial tests on mechanical properties of calcareous sand under various stress paths. *Chin. J. Geotech. Eng.* **2021**, *43*, 593–602.
41. Wang, Q.; Kong, Y.; Zhang, X.; Ruan, Y.; Chen, Y. Mechanical Effect of Pre-consolidation Pressure of Structural Behavior Soil. *J. Southwest Jiaotong Univ.* **2016**, *51*, 987–994.
42. Bao, S.; Wang, Q.; Bao, X. Study on Dispersive Influencing Factors of Dispersive Soil in Western Jilin Based on Grey Correlation Degree Method. *Appl. Mech. Mater.* **2013**, *291–294*, 1096–1100. [[CrossRef](#)]
43. Zhang, X.; Wang, Q.; Li, P.; Wang, R. Research on soil dispersion of Qian’an soil forest. *J. Northeast. Univ. (Nat. Sci.)* **2015**, *36*, 1643.
44. Han, Y.; Wang, Q.; Wang, N.; Wang, J.; Zhang, X.; Cheng, S.; Kong, Y. Effect of freeze-thaw cycles on shear strength of saline soil. *Cold Reg. Sci. Technol.* **2018**, *154*, 42–53. [[CrossRef](#)]
45. *ASTM D2487-11*; Standard Practice for Classification of Soils for Engineering Purposes (Unified Soil Classification System). ASTM International: West Conshohocken, PA, USA, 2011.

**Disclaimer/Publisher’s Note:** The statements, opinions and data contained in all publications are solely those of the individual author(s) and contributor(s) and not of MDPI and/or the editor(s). MDPI and/or the editor(s) disclaim responsibility for any injury to people or property resulting from any ideas, methods, instructions or products referred to in the content.